JOURNAL OF SOLID STATE CHEMISTRY 95, 14–20 (1991)

Anomalous Electronic Behavior in the Layered Halides Pr_2X_5 (X = Br,I)

H.-JÜRGEN MEYER* AND ROALD HOFFMANN†

†*Department of Chemistry and Materials Science Center, Cornell University, Ithaca, New York 14853-1301; and* **Institut für Anorganische Chemie, Universität Hannover, Callinstr.9, 3000 Hannover 1, Federal Republic of Germany*

Received February 28, 1991; in revised form May 24, 1991

For a number of lanthanide halides the unusual composition M_2X_5 (M = La,Ce,Pr; X = Br,I) has been achieved and confirmed by X-ray structures. Pr_2X_5 was found to be weakly semiconducting (Pr_2Br_5, 3800 Ω · cm; Pr_2I_5, 1600 Ω · cm at room temperature). An extended Hückel calculation of the band structure shows two narrow low-lying d bands, half occupied by two electrons per Pr_4X_{10} unit cell. These electrons may be considered localized as Mott insulating states. A detailed consideration of the paradoxical electric and magnetic properties of these materials is presented. The stabilizing effect of a hydrogen atom for the hypothetical $H_xPr_2Br_5$ ($x \leq 1$) is discussed.

Introduction

Diiodides are known almost for the whole lanthanide series. The electron configuration of LaI_2,CeI_2,PrI_2 (five phases) (*1*) and GdI_2 seems to be $f^{n-1}d^1$, and LaI_2 has been reported to be metallic (*2*). The $f^nd^0 \rightarrow f^{n-1}d^1$ configuration crossover (*3*) occurs at the beginning of each half-period of the rare earth metals, where the f-band is the highest in energy.

The diiodides that follow, such as NdI_2 and TmI_2, remain d^0 insulators. We note her that the border line of the interconfiguration crossover (interconfiguration fluctuation, ICF) occurs between PrI_2 (f^2d^1) and NdI_2 (f^4d^0).

Pr_2Br_5 and Pr_2I_5 (*4–7*) are obtained as bronze-colored rods with metallic luster, isostructural with La_2X_5 and $Ce_2X_5^8$ (X = Br,I). Consistent with what is known of their corresponding diiodides, two extra electrons of $Pr_4X_{10} \cdot 2e^-$ may be considered to occupy d states. The structures of Pr_2Br_5 and Pr_2I_5 have been confirmed and their physical properties have been studied in detail (*9*). Unexpectedly, the $5d^1$ Pr_2Br_5 and Pr_2I_5 are semiconductors, or almost insulators, with a room temperature bulk resistivity of 3800 Ω · cm and 1600 Ω · cm, respectively.

The electronic situation in the d^1 compounds RE_2X_5 obviously differs much from the parent d^1 REX_2 (X = Br,I) (*9*) halides. Our intention is to explore the anomalous electronic behavior of Pr_2Br_5 through electronic structure calculations using the extended Hückel (*10*) approach.

The Structure of Pr_2Br_5 (RE_2X_5: RE = La,Ce,Pr; X = Br,I)

Pr_2Br_5 crystallizes monoclinic ($P2_1/m$, $Z = 2$, $a = 778.76(8)$pm, $b = 416.57(5)$pm, $c = 1333.5(2)$pm, $\beta = 90.993(8)^\circ$) (*5, 8*),

0022-4596/91 $3.00

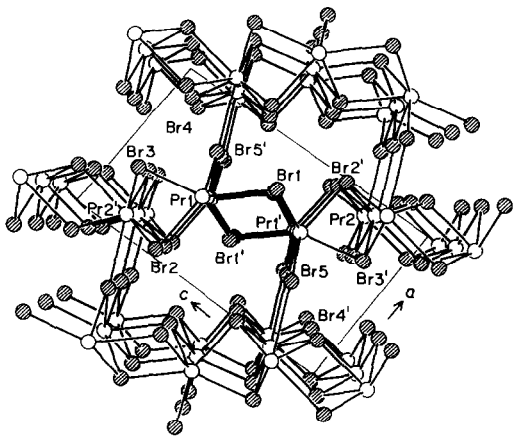

FIG. 1. Perspective view of the Pr_2Br_5 structure along the b-axis.

forming the layered structure shown in Fig. 1. The metal atoms form zig–zag layers which may be considered as derived from a hexagonal layer. The shortest metal–metal distances are obtained along the b repeat (416.6 pm), and between the two crystallographically distinct Pr atoms (421.0 pm). These separations are still well above the interatomic distance in Pr metal (365 pm), but only slightly longer than in the trans-edge-sharing octahedral Pr_4I_5Z (Z = Co, Ru,Os) cluster (391.0–404.1 pm) (*11*). The inversion-related Pr counterparts in each layer are separated by 489.0 and 494.2 pm, respectively. Metal bromide distances range from 295.7 to 313.1 pm, except for the longer Pr2–Br5 bridge (345.9 pm) between adjacent layers. This gives Pr2 a higher coordination number (CN = 8) compared with Pr1 (CN = 7). The Pr atoms exhibit distorted monocapped (Pr1) and bicapped (Pr2) trigonal prismatic Br coordination spheres. The average Pr2–Br distance is 308 pm; Pr1–Br, 300 pm.

Electronic Structure

The coordination environment around the two Pr atoms is mono- or bicapped trigonal prismatic. For c/a ratios bigger than one, the expected d orbital splitting in a trigonal prism is (d_{xy}, $d_{x^2-y^2}$) below d_{z^2} below (d_{xz}, d_{yz}). This is shown at left in Fig. 2, for a model $PrBr_6$ cluster (c/a ratio approximately 1.2). For c/a ratios smaller than one, the d_{z^2} orbitals are below the (d_{xy}, $d_{x^2-y^2}$) levels. Stabilization of the d_{z^2} level relative to the (d_{xy}, $d_{x^2-y^2}$) states is also obtained by introducing face-capping ligands. One or two capping ligands, however, break the degeneracy of the e sets, destabilize some orbitals, and introduce substantial mixing. Figure 2 also shows the corresponding levels for $PrBr_7$ and $PrBr_8$ model clusters, with geometries modeled after the Pr_2Br_5 structure. The lowest (d_{z^2}, d_{xy}) level would be a pure d_{z^2} state, were a third face-capping ligand introduced and geometrical adjustment made to reach a D_{3h} geometry. In each case we have chosen the z-axis along the approximate C_3 prism axis.

Note the expected ligand field pattern—three orbitals below two in the six-

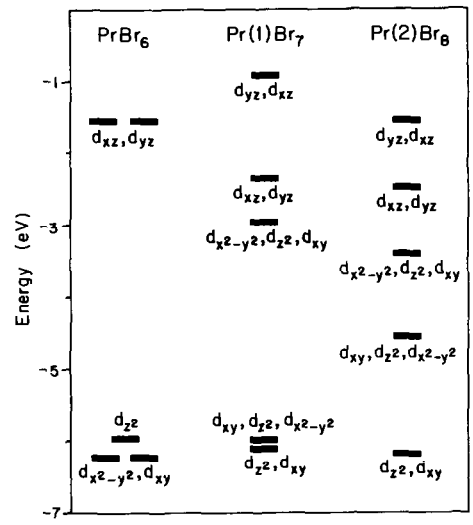

FIG. 2. Schematic d-block splitting diagram for a $PrBr_6$ trigonal prism (with c/a = 1.2) and the Pr(1)Br_7 and Pr(2)Br_8 subunits of the Pr_2Br_5 structure. d orbitals which contribute more than 15% to each orbital are listed. In each case the z-axis coincides with the pseudo-C_3 axis of the trigonal prism.

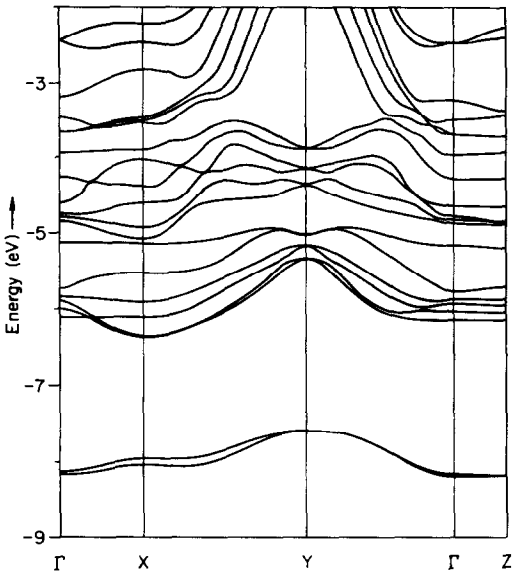

FIG. 3. Band structure for Pr_2Br_5 (Γ = 0,0,0; X = $a^*/2,0,0$; Y = $0,b^*/2,0$; Z = $0,0,c^*/2$). Two electrons occupy the two low-lying bands.

coordinate structure, two below three in the seven-coordinate one, and only one nonbonding level in the eight-coordinate geometry.

In the extended structure we could expect similar electronic features, because the Pr atoms are relatively far from each other. Any interaction between the Pr atoms, however, will affect the local ligand field splitting and thereby introduce additional orbital mixing.

Critical to our analysis are the lowest d bands of Pr, to be occupied by a total of two electrons. With four Pr atoms in the unit cell, two eight-coordinate and two seven-coordinate, we would expect six low-lying d bands. In fact the band structure of the three-dimensional material (Fig. 3) shows only two such low-lying bands per unit cell. In an attempt to trace the origins of the splitting off of two bands, we calculate a two-dimensional Pr_4Br_{12} slab, as well as one-dimensional chains containing separately Pr1 and Pr2 in their respective Br environments, and a one-dimensional Pr_2Br_8, containing both Pr1 and Pr2. There is some small Pr–Pr interaction lowering one band per Pr_2Br_5 unit in energy. This occurs first in the case of the one-dimensional Pr_2Br_8 double chain. This splitting is significant even in a molecular dimer model, Pr_2Br_{13}, reflecting that not only metal interactions of Pr1–Pr2 pairs, but also of metal atoms stacked along the b-axis introduce orbital mixing. The composition of the low-lying isolated band in the one-dimensional double chain is 59% Pr1, 33% Pr2, with most of the electron density occupying the Pr1 d_{z^2} (19%), d_{yz} (14%), d_{xz} (13%), d_{xy} (11%), and the Pr2 d_{xy} (20%) and d_{z^2} (11%) orbitals (the d_{z^2} orbitals in this chain, as well as in the extended structure, are parallel to [010]).

In the band structure of Fig. 3 there may be seen some degeneracies at special points in the Brillouin zone, for instance at Y, due to the 2_1 screw axis along b.

The bonding in the extended structure was analyzed with the aid of densities of states (DOS) (*10*) and crystal orbital overlap populations (COOP) (*10*). Figure 4 shows the contribution of Pr to the total DOS. The Pr–Br bonding comes mainly from Pr 5d and Br 4p interactions in the main Br 4p band between -12 and -15 eV, some from Br 4s interactions at around -23 eV. Due to this interaction the original d-block of the metal part of the lattice, centered between -6 and -9 eV, is raised and splits into two. The lower, narrow block, located around -8.0 eV, is mainly Pr d_{z^2} with admixture of d_{xz} and $d_{x^2-y^2}$ orbitals. We have already discussed the origin of these important bands. They are localized on Pr1 (61%) and Pr2 (31%) and their orbital contributions are: d_{xz} (24%), d_{z^2} (20%), $d_{x^2-y^2}$ (7%) and $d_{x^2-y^2}$ (16%), d_{z^2} (7%), d_{xy} (6%). Note the resemblance of this composition to that of a model dimer discussed above.

How many electrons are to be put into these bands? If we assume 2f electrons for

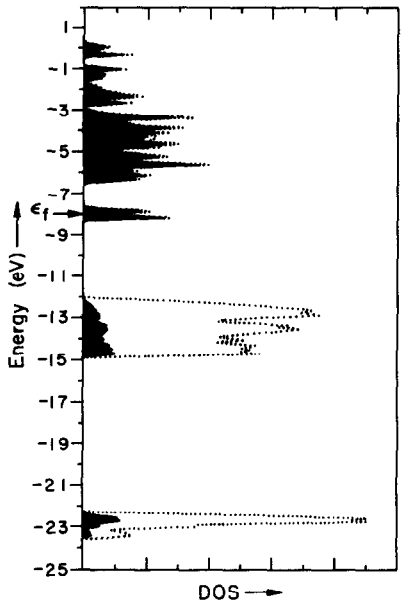

FIG. 4. DOS (density of states) projection. Contribution of Pr (5*d*, 6*s*, 6*p*) to the total DOS. The Fermi level for the low-spin arrangement is indicated by an arrow.

each Pr, this would make 8 *f* electrons per four Pr atoms. In the $(Pr_2Br_5)_2$ unit cell we are left with 10 electrons per four Pr, which leads to 2 electrons per four Pr to be put into the *d* band. Thus the group of two low-lying bands, with room for 4 electrons, would be half occupied.

We have to point out that there is no evidence for a mixed valence state ($4f^2$ Pr^{3+}, $4f^3$ Pr^{2+}) in Pr_2Br_5 from the crystal structure, nor from XANES studies (*8*). The 4*f* states were included in the calculation (not shown in the DOS). Their interactions with other orbitals were negligible, so that 28 *f* bands remained within an energy range of 0.17 eV (located at about −10 eV).

We would expect metal–metal bonding to be limited, due to the small number of electrons in these states. Nevertheless, there is some metal–metal interaction, indicated by the COOP curves (Fig. 5), and presaged by the level splitting pattern discussed above. The integration of all metal–metal interactions up to the fermi level reveals two positive overlap populations, namely between Pr1 and Pr1 in the direction of the *b*-axis (0.024) and between Pr1 and Pr2 (0.036). The latter are consistent with the shorter metal contacts. However, the remaining short contact between Pr2 and Pr2, parallel to the *b*-axis, is characterized by a slightly antibonding (−0.013) overlap population. If we take these bond indices seriously, this changes the simplified picture of metal ribbons running along *b* (Fig. 6b) (based on the shorter Pr–Pr contacts) toward a model of corner sharing metal triangles along *b* (Fig. 6c). It is clear that these metal–metal overlap populations are small on an absolute scale, but as we have noted before, they introduce significant orbital mixing.

Returning to the two low-lying *d* bands, we note that their dispersions are not large and their splitting always small, maximally 0.13 eV. Thus high-spin or low-spin electron arrangements may not differ much energetically ($\Delta < 5$ kT). Both cases, however,

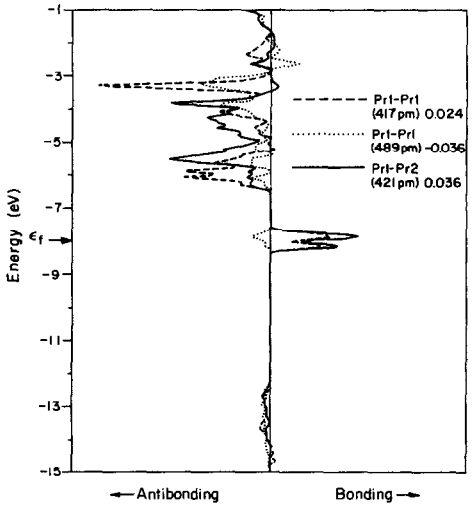

FIG. 5. COOP (crystal orbital overlap population) curves of the metal–metal interactions in Pr_2Br_5.

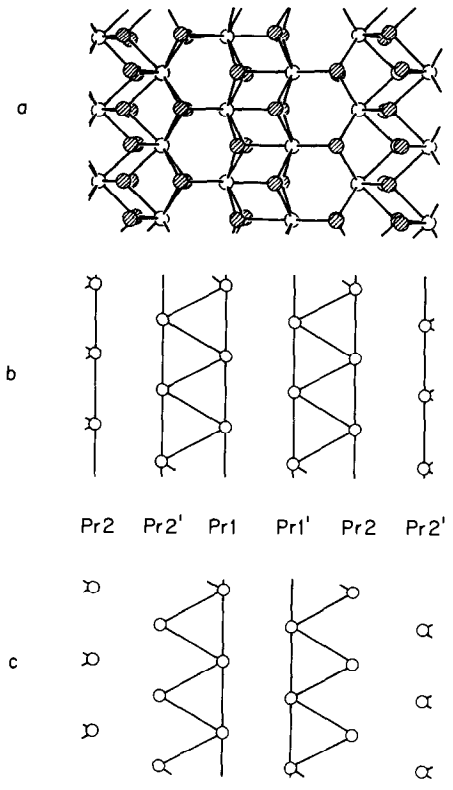

FIG. 6. (a) Perspective (101) projection of a section of one layer in the Pr_2Br_5 structure. (b) Metal part of the layer only. Metal–metal distances less than 430 pm are outlined. (c) Metal part of the layer only. All positive overlap populations are outlined.

should represent metallic states, unless electrons are localized.

Electron Localization

One basic argument for localized states is the appearance of large lattice spacings between atoms. For a widely spaced system, as for a collection of quasi-isolated atoms, electrons should be assigned to lattice sites. A clearly insulating state is the result. The metal–metal distances obtained in Pr_2Br_5 are no shorter than 417 pm. Only if the metal–metal distances were sufficiently short would increased *d* interactions lead to a broadening of the *d*-block, which, in the extreme, could then reach the *f* bands.

In Pr_2Br_5 the *d*-block dispersion is due mainly to the ligand field splitting, with two narrow bands containing two electrons split off. The perturbation that can induce a high-spin state is the Coulomb repulsion. This, however, cannot be evaluated from a one-electron picture of the type used in the extended Hückel approach. Taking electron–electron interactions such as the on-site electron repulsion into consideration the situation becomes different. If the bandwidth gap is sufficiently small compared to the on-site electron repulsion the high-spin state becomes more stable and electrons are localized on lattice sites. These states are insulating in nature or show weak thermally activated electron hopping. But electron hopping from one site to another leads to a situation where two electrons reside on a single site, thereby causing on-site repulsion.

Such insulating states resulting from partially filled bands are referred to as Mott–Hubbard localized states (*12*).

In contrast, a low-spin situation should lead to a metallic state. This is not observed in the conductivity experiment, nor indicated by the magnetic data. The susceptibilities of Pr_2Br_5 and Pr_2I_5 exhibit paramagnetic behavior below 300 K (3.47 BM, 3.30 BM per Pr^{3+}), consistent with values for Pr^{3+} (3.58 BM) (*13*), and antiferromagnetic ordering at T_N = 50 K and T_N = 37 K, respectively.

Mott insulators are characterized by partially filled narrow levels, as obtained in the present band structure calculation. Furthermore, the COOP values noted above raise the possibility of electron localization in triangular interstices build up by the two crystallographically distinct Pr atoms, forming corner-sharing triangles parallel to the *b*-axis. With the present electron count, one electron could occupy a three-center orbital of the non-bro-

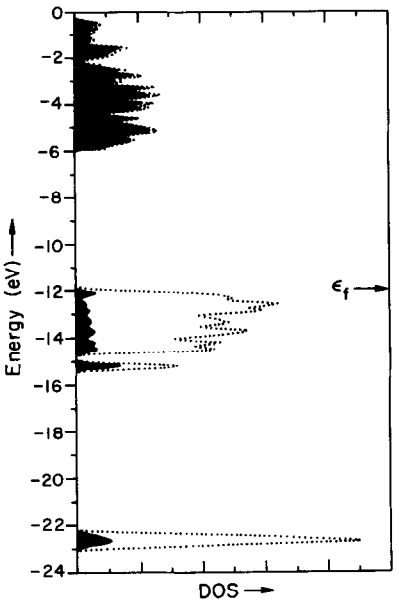

FIG. 7. DOS of the hypothetical HPr_2Br_5 structure.

mide-capped praseodymium triangles. The bonding and thus the nature of these three-center orbitals may result mainly from orbital mixing of d_{z^2} orbitals (z along the crystallographic b-direction) with d_{xz} orbitals. Two electrons in each triangle would be sufficient for three-center-two-electron bonding. It should be noted that such semilocalized binding in extended systems has been recently suggested for MoS_2, $H_x(Nb, Ta)S_2$ and ZrS by Yee and Hughbanks (*14*). The reader is referred to their work to see how such a localization may be implemented.

There is another interesting possibility that merits consideration. A stabilizing effect might be obtained by introducing hydrogen atoms into the non-halide-capped metal triangles, yielding Pr–H distances of 242 pm with the composition $H_xPr_2Br_5$ ($x \leq 1$). For this hypothetical compound the two low-lying d bands will be drastically lowered below the Br p-block, as shown in Fig. 7, forming the bonding Pr–H combination. The Pr–H antibonding (empty) combination is raised far above the d-block.

Conclusion

Compounds with d^1 configuration usually appear to be metals or semiconductors. Interestingly, both Pr_2Br_5 and Pr_2I_5 are insulators, which is not expected from their $5d^1$ configuration. The electronic characteristics of Mott–Hubbard insulators are influenced by intraatomic interactions and crystal-field splitting of the $3d$ levels. This was studied by us for the Pr_2Br_5 case. As a result of large metal separations in the structure, only weak d interactions are present between the metal atoms. With two narrow half-filled valence bands, both compounds can be viewed as Mott insulators, with some proximity of localized electrons in Pr triangles of the metal layer. These metal triangles, referred to as electron hosts, are all uncapped, of the pseudo-hexagonal layer, while the remaining triangles are capped by two bromide (iodine) atoms from above and below. The antiferromagnetic and paramagnetic properties of Pr_2Br_5 and Pr_2I_5 below and above T_N are also typical of Mott insulators (*14*).

The hexagonal layered structure of (Nb, Ta)S_2 (d^1) takes up hydrogen to form $H_x(Nb,Ta)S_2$ (*16*), where hydrogen is located in triangles of the hexagonal metal plane. A similar incorporation of hydrogen might be possible for Pr_2Br_5.

The electronic structure of some other RE halides seems rather complicated, and distinct from the present M_2X_5 case. $Pr_{0.3}PrCl_3$ (*17*) may be viewed as containing some extra Pr in interstices of distorted octahedral halide coordination of the $PrCl_3$ lattice, which has the UCl_3 structure. The compound does not show a phase width. Introducing partially filled d-states, $(Pr_{0.3})^{3+}$, may not change, however, the insulating behavior, since metal–metal

distances are still large (441 pm). In contrast, $Nd_{0.3}NdCl_3$[18] was reported as a mixed valence compound with $4f^4(Nd^{2+})$ and $4f^3(Nd^{3+})$ states. The latter usually can be derived by the associated reduction in cationic radius with increase of the formal valence from 2+ to 3+.

Appendix

The extended Hückel tight-binding method was used (*19*). H_{ii} values for Pr were obtained from self-consistent charge iteration on Pr_2Br_5 (6*s*, −7.42 eV; 6*p*, −4.65 eV; 5*d*, −8.08 eV). Because *f* orbital energies and parameters were not available for Pr, we used the values of Sm, whereas the H_{ii} value for Pr was chosen to be −10 eV (H_{ii}(Sm) = −11.28 eV) (*20*), considering the trend in the RE metal series. DOS curves were calculated using a set of 54 k points for the irreducible wedge of the Brillouin zone. The band structure was calculated for all special points of the monoclinic Brillouin zone. Figure 3, however, shows only a representative section.

Acknowledgments

H.-J. Meyer thanks Dr. K. Krämer and Prof. G. Meyer (Universität Hannover, FRG) for providing data on Pr_2Br_5 and Pr_2I_5. The work at Cornell was supported by the National Science Foundation through Research Grants CHE-8912070 and DMR 8818558.

References

1. E. Warketin and H. Bärnighausen, *Z. Anorg. Allg. Chem.* **459** 187 (1970).
2. J. H. Barrow, C. H. Maule, P. Strange, J. N. Tothill, and J. A. Wilson, *J. Phys. C Solid State Phys.* **20,** 4115 (1987); J. D. Corbett, R. A. Sallach, and D. A. Lokken, *Adv. Chem. Ser.* **71,** 56 (1967).
3. J. A. Wilson, *Struct. Bond.* **32,** 57 (1977).
4. R. A. Sallach and J. D. Corbett, Inorg. Chem. **2,** 457 (1963).
5. J. D. Corbett, L. F. Druding, W. J. Burkhard, and C. B. Lindahl, *Discuss. Faraday Soc.* **32,** 79 (1961).
6. T. Schleid and G. Meyer, *Z. Anorg. Allg. Chem.* **552,** 97 (1987).
7. E. Warkentin, Dissertation, Karlsruhe, FRG (1977).
8. K. Krämer, Th. Schleid, M. Schulze, W. Urland, and G. Meyer, *Z. Anorg. Allg. Chem.* **575,** 61 (1989); K. Krämer and G. Meyer, *Eur. J. Solid State Inorg. Chem.* **28,** 523 (1991).
9. K. Krämer, G. Meyer, P. Fischer, A. W. Hewat, and H. U. Güdel, *J. Solid State Chem.* **95,** 1 (1991).
10. R. Hoffmann, *Angew. Chem.* **99,** 871 (1987); *Angew. Chem. Int. Ed. Engl.* **26,** 846 (1987); T. Hughbanks and R. Hoffmann, *J. Am. Chem. Soc.* **105,** 1150 (1983); R. Hoffmann, "Solids and Surfaces," VCH Publishers, New York (1988).
11. M. W. Payne, P. K. Dorhout, and J. D. Corbett, (submitted for publication, *Inorg. Chem.*).
12. N. F. Mott, "Metal-Insulator Transitions," Barnes and Noble, New York (1977).
13. C. Kittel, "Introduction to Solid State Physics," 6th ed., p. 405, J. Wiley, New York (1986).
14. K. A. Yee and T. Hughbanks, *Inorg. Chem.*, **30,** 2321 (1991).
15. J. Spalek, *J. Solid State Chem.* **24,** 2095 (1985).
16. D. Murphy and G. W. Hull, *J. Chem. Phys.* **62,** 967 (1975).
17. G. Meyer, T. Schleid, and K. Krämer, *J. Less-Common Met.* **149,** 67 (1989).
18. A. Lumpp and H. Bärnighausen, *Z. Kristallogr.* **182,** 174 (1988).
19. R. Hoffmann and M.-H. Whangbo, *J. Am. Chem. Soc.* **100,** 6093 (1978); M.-H. Whangbo, R. Hoffmann, and R. B. Woodward, *Proc. R. Soc. London,* **A366,** 23 (1979); R. Hoffmann, *Rev. Mod. Phys.* **60,** 601 (1988).
20. J. V. Ortiz and R. Hoffmann, *Inorg. Chem.* **24,** 2095 (1985).